UDC 524.74:524.82 *Astrofiz. Issled. (Izv. SAO)*, 1993, **35**, 6-75

AN EVIDENCE FOR ENHANCED STAR FORMATION RATE IN IRAS-DETECTED ARAKELIAN GALAXIES

I.M. YANKOULOVA, V.K. GOLEV,
Department of Astronomical Observatory, University of Sofia,
5 Anton Ivanov St., 1126 Sofia, Bulgaria

G.T. PETROV
Department of Astronomy and National Astronomical Observatory,
Bulgarian Academy of Science, 72 Lenin Blvd., Sofia, Bulgaria

Received May 5, 1991

ABSTRACT. *The IR emission of 182 Arakelian galaxies (AKN), included in the IRAS Survey, is considered as an evidence of enhanced star formation rate (SFR) in them. About 63% of the AKNs have far infrared luminosities ($\geq 10^{44}$ erg·s^{-1}) in 1-500 μm IR spectral band. The distribution of log (f_{60}/f_{100}), peaked at about 45 K, shows that IRAS AKNs are considerably warmer than "normal" S galaxies. IRAS AKNs have a tendency to extend the relation f_{100}/f_{60} vs L_{IR}/L_B for "normal" S galaxies. They emit IR energy in 40-100 μm band up to seven times more than in optics. The mean ratio $< L_{FIR}/L_B >$ for 148 IRAS AKNs with known redshifts is 3.63.*

It is suggested that there are two IR emitting components in the IRAS AKNs - a warm one connected with the UV-fluxes of the new-born massive stars, reradiated by dust, and a cool one, originated from the dust in galactic disks and heated by the general interstellar radiation field. The warm IR luminosities and warm IR fractions are determined on the basis of IR color-color diagrams α(25/12), α(60/25), and α(100/60). The mean warm IR fraction is 0.55 when the grain mass absorption coefficient model with n=1.0 is used (or 0.72 if n=0.0 is adopted).

The dust mass responsible for IR flux at 60 μm is derived to be about $10^5 \mathfrak{M}_\odot$, assuming the dust clouds are optically thin, and using the dust temperature $T_d \approx 36$ K (deduced from the f_{60}/f_{100} ratio).

There is a relation between L_{IR} and L_B which points out that the most

IRAS AKNs have rather enhanced SFR.

ИК-излучение 182 Аракеляновских галактик (AKN), содержащихся в обзоре IRAS, рассматривается в качестве доказательства повышенного темпа звездообразования (SFR) в них. Около 63% AKN показывают высокие ИК-светимости ($\geq 10^{44}$ erg s^{-1}) в диапазоне 1-500 мкм. Распределение log (f_{60}/f_{100}) галактик IRAS-AKN имеет максимум около ~45 К - и показывает, что эти галактики значительно теплее, чем "нормальные" S-галактики. Галактики IRAS-AKN расширяют в сторону больших величин зависимость между f_{100}/f_{60} и L_{IR}/L_B для "нормальных" спиралей. Они излучают в диапазоне 40-120 мкм до 7 раз больше, чем в оптическом. Среднее отношение $\langle L_{FIR}/L_B \rangle$ для 148 галактик IRAS-AKN с известными красными смещениями составляет 3.63.

Мы предполагаем, что в галактиках IRAS-AKN существуют две компоненты, излучающие в ИК-области: горячая, связанная с УФ-потоком от новорожденных массивных звезд, переизлученным пылью, и холодная, порожденная пылью в галактических дисках, нагреваемой общим межзвездным радиационным полем. Основываясь на цветовых диаграммах в ИК-области $\alpha(25/12)$, $\alpha(60/25)$, и $\alpha(100/60)$, мы нашли параметры составляющих ИК-излучения для этих галактик. Доля теплой ИК области составляет 0.55, если используется модель для коэффициента поглощения с n = 1 (или 0.72, если n = 0).

Мы определили массу пыли, ответственной за ИК-излучение на 60 мкм, принимая температуру пыли $T_d \approx 36$ К (найденную из f_{60}/f_{100}). В предположении о малой толщине облаков эта масса порядка 10^5 $M_\odot$.

Существует зависимость между L_{IR} и L_B, которая показывает, что темп звездообразования в галактиках IRAS-AKN действительно является повышенным и многие из них являются галактиками типа starburst.

1. INTRODUCTION

Surveys widely carried out in the last decades in optics have produced large sets of emission-line galaxies (ELGs). In the majority of the observed galaxies with emission lines in their spectra the line emission probably is an indicator of gas photoionized by hot, young stars associated with the regions of active star formation. On the other hand, most of the energy emitted by such stars at short optical wavelengths is actually detected as reradiated by dust far-infrared (FIR) emission. That is why, as have been noticed by Salzer and MacAlpine (1988) (hereafter their paper is referred to as SM), the investigation of the FIR properties of samples of optically selected ELGs is important for gaining a better knowledge of the energetics of these galaxies, as well as for understanding the galaxy activity, both AGN-like and induced by star-formation processes. The use of the database accumulated by *Infrared Astrono-*

mical Satellite (IRAS) provides the best opportunity to select subsets of ELGs with well manifested FIR properties.

One of the optical surveys carried out, which is not so popular as those of Markarian and University of Michigan for example, is the list of Arakelian galaxies (AKNs) (Arakelian, 1975). This survey contains 591 galaxies with relatively high surface brightness (brighter than 22 mag·arcsec^{-2} in Zwicky photographic magnitude system). More than half of AKNs (about 300 objects) show both the emission lines in their optical spectra and excess in radio-flux at 408 MHz (Arakelian, 1975). There are some evidences that the high optical surface brightness of AKNs may be caused by the larger abundance of young and blue stars or by their compactness. Both these reasons may be responsible for more intensive general radiation field.

The present work considers the infrared radiation of a sample of 182 AKNs included in *Cataloged Galaxies and Quasars Observed in the IRAS Survey* (Lonsdale et al., 1985) which contains about 31% of the whole Arakelian's list. 148 of *IRAS*-detected AKNs have known redshifts, and 35 of them have well determined *IRAS* fluxes.

2. GENERAL PROPERTIES

We assume that the infrared radiation of the galaxies in question is due to dust thermal reradiation of the stellar radiation field.

As indicators of the "infrared activity" of galaxies the IR luminosities L_{IR} and the ratio L_{IR}/L_B may be used, where L_B is taken to be equal to νf_ν at λ=4400 Å. We have used the calibration of Houck et al. (1984) in the blue region f_B:

$$\log f_B = -7.54 - 0.4\, m_p, \qquad (1)$$

where f_B is expressed in Wm^{-2} and m_p is the apparent photographic magnitude from *Catalogue of Galaxies and Clusters of Galaxies* (CGCG - Zwicky et al., 1961-1968). Note that these fluxes are about 5 times larger than those in standard B-filter (Soifer et al., 1987).

2.1. Infrared luminosities and colors

Infrared fluxes f_{IR} refer to the infrared emission between 40 and 120 μm which is determined according to Dennefeld et al. (1985):

$$f_{IR} = 1.75\ (2.55\ f_{60} + 1.01\ f_{100})\ 10^{-14}\ Wm^{-2}, \qquad (2)$$

where f_{60} and f_{100} are the *IRAS* cataloged flux densities in Jy. We have used Eq.(2) in order to compare our results with those of other authors for different kinds of objects.

Following Belfort et al. (1987), we have estimated the total far infrared emission

f_{FIR} from about 1 to 500 μm the expression

$$f_{FIR} = 1.75\ (12.66\ f_{12} + 5.0\ f_{25} + 2.55\ f_{60} + 1.01\ f_{100})10^{-14}\ Wm^{-2}. \quad (3)$$

The distribution of the total FIR luminosities L_{FIR} for a sample of *IRAS*-detected AKNs with known redshifts (consisting of 148 objects) is shown in Fig. 1. All the luminosities, L_B, L_{IR}, L_{FIR}, have been computed assuming a pure Hubble flow with $H_0 = 75$ km/s/Mpc and $q_0 = 1.0$. It should be noted that about 63% of all *IRAS*-detected AKNs have $L_{FIR} \geq 10^{44}$ erg/s. In fact this means that these AKNs belong to ELIRS (extremely luminous far infrared sources - see Harvit et al., 1987) because they have both strong IR radiation within 1-500 μm band and low-ionized optical spectra.

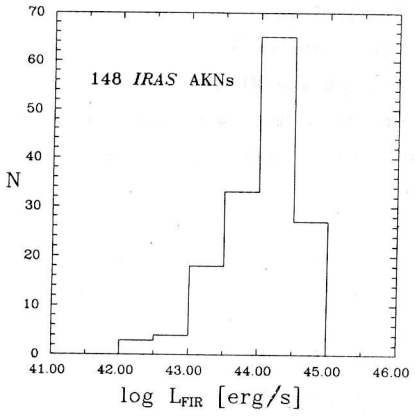

Fig. 1. *Distribution of the total FIR luminosity of all 148 AKNs with known redshifts found in the IRAS Point Source Catalog.*

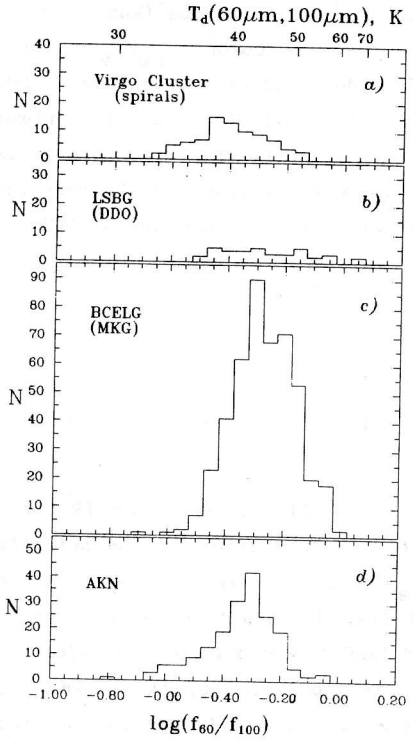

Fig. 2. *Distributions of the f_{60}/f_{100} ratio of four different samples of IRAS-detected galaxies: (a) "normal" spirals in Virgo cluster, (b) galaxies with low surface brightness labeled as LSBG, (c) blue compact emission line galaxies labeled as BCELG, and (d) all 182 IRAS-detected AKNs discussed here.*

Fig. 2d shows the distribution of the color index ratios f_{60}/f_{100} for our sample of 182 *IRAS*-selected AKNs. For the sake of comparison the same distributions for three other samples of galaxies are also presented in Fig. 2. These are the distribu-

tion of "normal" spirals in Virgo cluster, the distribution of galaxies with low surface brightness (LSBG - see Helou, 1985), and the distribution of blue compact emission line galaxies (BCELG) picked out from the Markarian lists (Kunth and Sevre, 1985). On this diagram the lower horizontal axis is labelled with log (f_{60}/f_{100}). On the upper horizontal axis of Fig. 2 the corresponding color temperature is marked when $f_\nu \sim \nu^n B_\nu(T)$ and $n=0$ grain absorption model is accepted.

The mean infrared color for the sample of 148 *IRAS*-detected AKNs with known red shifts is $\langle log(f_{60}/f_{100})\rangle=-0.34$ and the mean ratio $\langle L_{IR}/L_B\rangle=1.32$. The corresponding values for the "normal" S galaxies are $\langle log(f_{60}/f_{100})\rangle=-0.43$ and $\langle L_{IR}/L_B\rangle=0.4$ (see de Jong et al., 1984). It may be seen that the *IRAS*-detected AKNs are warmer than the "normal" S galaxies, with distribution peaking clearly at $T \sim 45$ K. It can be seen also that the *IRAS* AKNs have a distribution of temperature color index f_{60}/F_{100} similar to that of the BCELGs (Kunth and Sevre, 1985).

The infrared colors f_{100}/f_{60} vs the indices of activity L_{IR}/L_B for the sample of 148 *IRAS*-detected AKNs with known redshifts are plotted in Fig. 3. On this diagram 35 objects with well determined *IRAS* fluxes at 60 and 100 μm are marked by circles. The region occupied by the "normal" S galaxies picked out from the Virgo cluster is outlined by a solid line. In the same Figure the BCELGs would have occupied the upper right part. Thus, *IRAS*-selected AKNs extend the same relation for the normal S galaxies (see Kunth and Sevre, 1985).

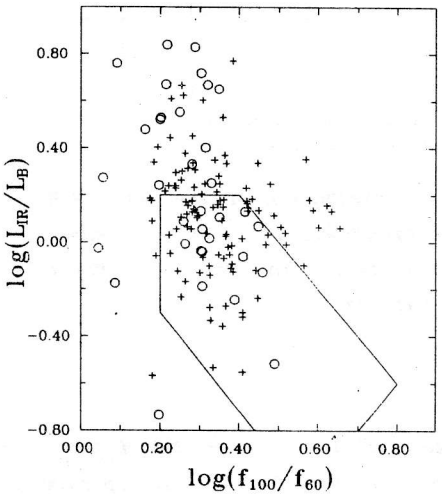

Fig. 3. *Relation between the IR color f_{100}/f_{60} vs the index of IR activity L_{IR}/L_B for all 148 IRAS AKNs with known redshifts. 35 objects with well determined IRAS fluxes are noted by circles. The region occupied by the "normal" S galaxies in Virgo cluster is outlined by solid line (Jong et al., 1984).*

The ratio f_{IR}/f_B has been adopted by many authors as a convenient measure of the infrared activity of galaxies. The mean ratio of 148 IRAS-selected AKNs with known redshifts is $\langle L_{FIR}/L_B\rangle=3.63$. In Fig.3 there is a tendency of increasing of the dust temperature derived from f_{100}/f_{60} and the galaxies become warmer with the IR activity (L_{IR}/L_B ratio). This has been already mentioned by de Jong et al. (1984) for the

"normal" S members of Virgo cluster. *IRAS*-detected AKNs tend to extend this relation and the BCELGs show the same tendency. At temperatures 40-50 K *IRAS*-detected AKNs emit up to seven times more energy in the infrared than in the optical blue band. It should be noted that the region occupied by *IRAS*-selected AKNs coincides with the one occupied by the BCELGs. This result probably points at higher star formation rate (SFR) in these galaxies than in normal spirals and irregular galaxies.

2.2. Dust masses

The IR emission of the dust is caused mainly by the dust component with low temperature (about 30 K for the cirrus emission). In the optically thin case the mass of the dust emitting at a given wavelength is determined as

$$\mathfrak{M}_{dust}(\lambda) = 4\pi r_g^2 f_\lambda / 4\pi B_\lambda(T_d) K_\lambda, \qquad (4)$$

where r_g is the distance to the galaxy, f_λ is the observed flux density at wavelength λ, T_d is the dust temperature, $K_\lambda = Q_\lambda/(4/3)\alpha\rho$ cm^2/g is the mass absorption coefficient, and $Q_\lambda \sim \lambda^{-n}$ is the absorption efficiency of the dust. We assume that the dust is a mixture of graphite and silicon particles with density ρ=2 g/cm^3, whose radii α are equal to 0.1 and 1.0 μm. We adopt n=1 and the corresponding mass absorption coefficients are based on the recent grain models of Drain and Lee (1984).

The dust masses generating the observed IR-flux at 60 μm have been obtained using Eq. (4), where the dust temperatures T_d were deduced only from f_{60}/f_{100} ratio if n=1 grain absorption model is adopted. By this way we found that the mean dust mass of *IRAS*-detected AKNs is $\mathfrak{M}_{dust}(60\ \mu m) \sim 10^5 \mathfrak{M}_\odot$.

A correlation might be expected between the ratio L_{IR}/L_B which characterizes the starburst activity and the dust mass radiating at 60 and 100 μm. Such a correlation for 148 *IRAS*-selected AKNs with known redshifts, if only the graphite grains of 0.1 mm are taken into account, is shown in Fig. 4. In fact this correlation is not seen clearly and its Pearson correlation coefficient is about 0.60.

2.3. Star formation rates

The star formation rate is considered from a point of view of the relation between L_{IR} and L_B (see Gallagher and Hunter, 1987). This relation for above mentioned 148 AKNs is presented in Fig. 5. Most of them are between the lines of constant SFR and starburst. Some of them are obviously below the latter. This indicates an increased SFR in the *IRAS*-detected Arakelian galaxies.

Following Gallagher and Hunter (1987), we can make a raw estimation of SFR:

$$d\mathfrak{M}/dt = 2.5 \cdot 10^{-10} \beta^{-1} \delta \cdot L_{FIR}\ \mathfrak{M}_\odot \text{ per year}, \qquad (5)$$

if the mass of the warm stars is near to 10 $\mathfrak{M}_\odot$. Here $\beta \sim 0.5$ and it depends both on the

new-born star effective temperature and on galaxy's geometry. The part δ of the infrared radiation, which is connected with the young stars, must be ≤ 1.0, and according to our estimation it is about 0.55 (n=1, dust grain absorption model adopted). As a result it was obtained $d\mathfrak{M}/dt \approx 8\ \mathfrak{M}_{\odot}$ per year.

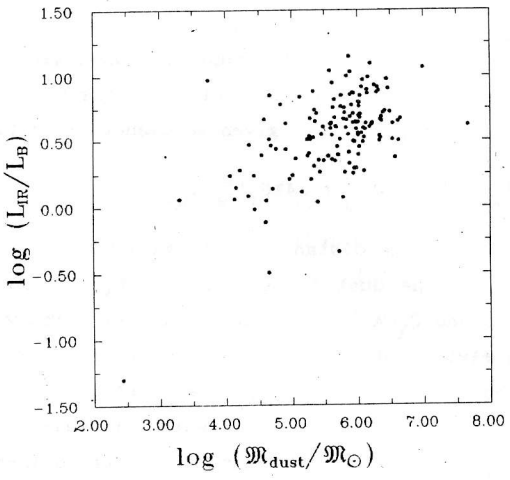

Fig. 4. *Correlation between the dust mass radiating at 60 μm (at T_d deduced only from f_{60}/f_{100} ratio and n=1 model) in solar mass units vs the L_{IR}/L_B ratio.*

3. RESULTS

The mean color temperature for the total sample of 182 *IRAS*-selected AKNs based on the f_{60}/f_{100} ratios is about 36 K and it differs from 185.5 K, the temperature based on the f_{12}/f_{25} ratios (all values are determined within the n=1 dust grain absorption model). So we may expect that the IR radiation generated by dust reradiation of the UV photons of new-born massive stars originates in two differently situated dust clouds. Following Hunter et al. (1986), and for convenience only, we will refer to them as the "near-dust" and "far-dust" IR components.

The "near-dust" IR component is connected with the radiation at 12 and 25 μm coming from hot dust located in (or at least very near) the HII regions situated around the new-born massive stars. The mean dust color temperatures, derived from the ratio f_{12}/f_{25}, concern these regions.

The "far-dust" IR component is related mainly to the radiation at 60 μm and less to that at 100 μm. This radiation arises in warm dust associated with neutral gas outside of the ionized gas region or in the associated neutral molecular gas clouds, out of which the HII regions have formed. The mean color temperatures, derived from the ratio f_{60}/f_{100}, concern the dust, which is essentially responsible for the "far-dust" IR component.

There is a third IR component which is cooler than the "far-dust" one. It origi-

nates from the dust in galactic disks heated by the general interstellar radiation. Thus, it resembles the "cirrus" radiation in our Galaxy. As in the Milky Way, we consider the dust temperature of this IR component to be about 30 K.

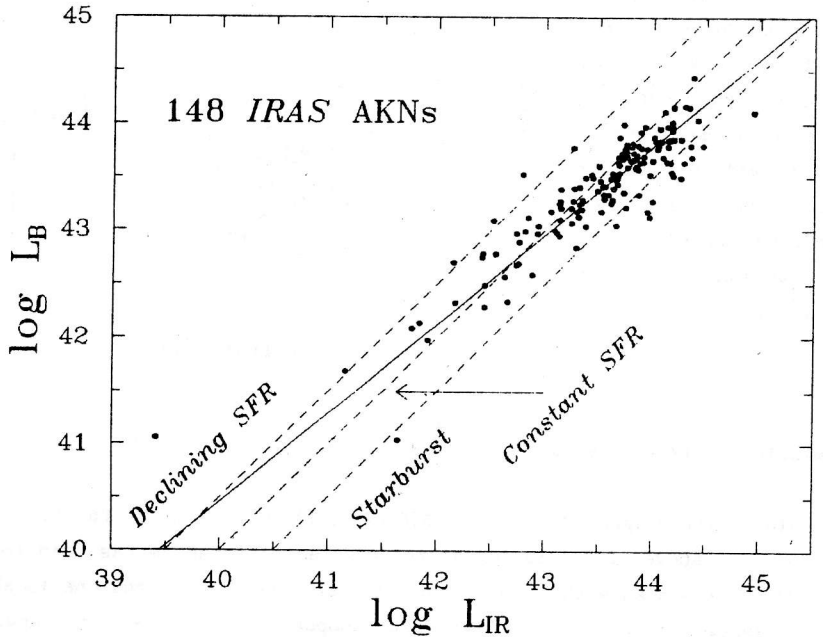

Fig. 5. *The IR luminosity L_{IR} between 40 and 120 μm vs the blue luminosity L_B (solid line). The lines of constant SFR, the starburst line and the line of declining SFR are superimposed as dashed lines according to Gallagher and Hunter (1987).*

3.1. Emission at 60 and 100 μm

As it was noted above, only 35 *IRAS*-selected AKNs have well determined IRAS fluxes. We include them in a separate subset sample. Their IR emissions have been assumed to be proportional to $\nu^n B_\nu(T)$ where $B_\nu(T)$ is a Plank function. Two black-body model spectrum has been adopted for the emission at 60 and 100 μm. There are the "cirrus" black-body radiation at 30 K, and the black-body emission of the warmer "far-dust" component, whose temperature is 50-120 K (Sekiguchi, 1987).

The IR color-color diagram α(60/25) vs α(100/60) for *IRAS* AKNs of the subset is shown in Fig. 6, where the loci of the two-black-body models have been plotted (α is the slope of power-law spectrum $f_\nu \sim \nu^\alpha$). The dust temperatures $T_W(60,100)$ and warm fractions at 60 μm, $fr^W_{60\mu m}$, and at 100 μm, $fr^W_{100\mu m}$, related to the "far-dust" component, have been determined from Fig. 6. These fractions for each galaxy of the subset are presented in Table 1.

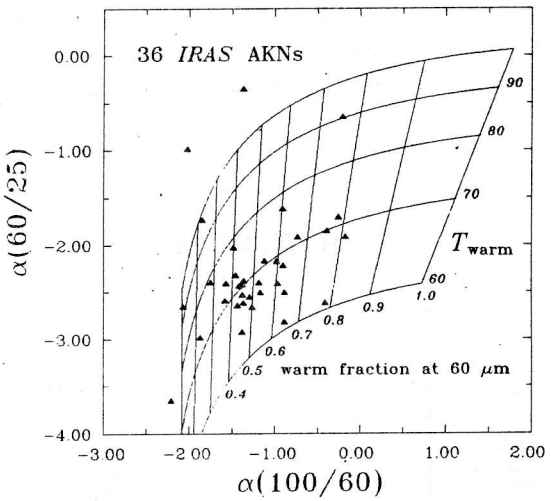

Fig. 6. *IR color-color diagram α(60/25) against α(100/60) for 35 IRAS-detected AKNs sampled in our subset. The right-hand line (where the temperature is marked) is formed only by the warm IR component. Along the two-temperature model curve the warm fractions at 60 μm* $fr^{W}_{60\mu m}$ *are given.*

3.2. Emission at 12 and 25 μm

The IR color-color diagram α(25/12) vs α(60/25), shown in Fig. 7, has been used in the same manner as above. The emission at the wavelengths $\lambda \leqslant 40$ μm has been formed as a sum of two black-bodies with two different temperatures. The first one is about 50 K and it is representative of the "far-dust" component. The other one ranges from 150 to 290 K and represents the influence of the hotter "near-dust" component (i.e. the IR emission of the galactic dust, which is located closely around the new-born massive stars). By means of Fig. 7 for each galaxy of the subset the temperature $T_W(12, 25)$ and the warm fraction at 25 μm, $fr^{W}_{25\mu m}$, relating to the "near-dust" IR component, have been determined. These quantities may be seen in Table 1 too.

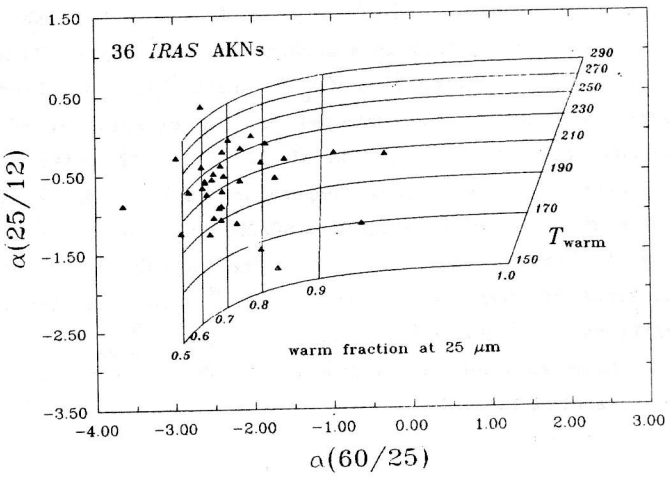

Fig. 7. *IR color-color diagram α(25/12) against α(60/25) for 35 IRAS-detected subset AKNs. As on the previous figure, the right-hand line is formed only by the warm IR component. Along the two-temperature model curve the warm fractions at 25 μm* $fr^{W}_{25\mu m}$ *are marked.*

Almost all of the emission at 12 and 25 μm is due to the warm IR emission. When the warm fractions $fr^{W}_{100\mu m}$, $fr^{W}_{60\mu m}$ and $fr^{W}_{25\mu m}$ at given wavelengths are known, then, by means of Eq.(3), the total warm IR luminosities L^{W}_{FIR} and the total warm IR fractions L^{W}_{FIR}/L_{FIR} have been calculated. All these quantities for *IRAS* AKNs, included in the subset, are presented in Table 1. The mean total warm IR fraction deduced is $\langle L^{W}_{FIR}/L_{FIR}\rangle = 0.55$ if n=1 model is used, and $\langle L^{W}_{FIR}/L_{FIR}\rangle = 0.72$ if n=0 is adopted.

There is a high correlation between the warm IR fraction and UV color U-B for *IRAS* AKNs of the subset. This correlation is shown in Fig. 8 and its Pearson correlation coefficient is about 0.9.

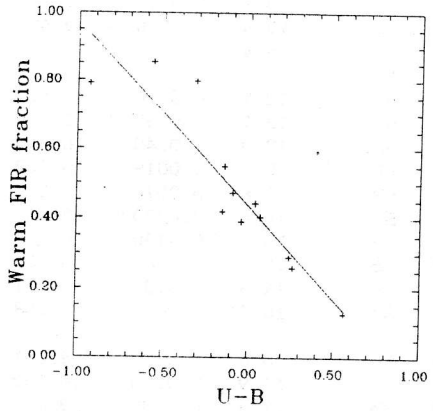

Fig. 8. *Correlation between the warm far-infrared fraction and the color U-B for the subset of IRAS-detected AKNs whose colors are available.*

As it is seen from Table 1, the larger part of the emission $f_{100}(1-fr^{W}_{100\mu m})$ at 100 μm is due to the cooler "cirrus" dust component, which is warmed up by the general interstellar radiation field. By means of the Eq.(4) the mean dust mass, responsible for the "cirrus" emission, has been found to be about $2\cdot10^{6}$ $\mathfrak{M}_{\odot}$.

Most of the emission at 60 μm for essential part of the galaxies in the subset originates in the "far-dust" component, which is connected with the neutral molecular gaseous clouds and the dust associated with neutral gas outside of the HII regions. The mass of this dust component for each subset galaxy has been obtained as above with temperatures $T_{W}(60,100)$ given in Table 1, and its mean value is about $1.5\cdot10^{4}$ $\mathfrak{M}_{\odot}$.

Table 1. IRAS-detected AKNs with well determined IR fluxes - the data

AKN	Type	m_p	z	$\log L_{FIR}/L_\odot$	$\log L_{FIR}/L_B$	$T_d(60/100)$ [K]	$T^W_{60,100}$ [K]
55	S pec	13.6	0.0190	10.891	-	-	-
77	S	13.2	0.0160	10.936	0.66	34.6	70.2
80	SB	15.2	0.0350	11.594	1.06	35.4	67.5
88	S pec	13.5	0.0150	11.039	0.93	37.8	66.0
89	SBa	13.9	0.0165	10.858	0.80	38.3	68.3
120	-	14.6	0.0330	11.000	0.65	35.0	120.0
136	-	12.5	0.0120	10.756	0.50	38.4	64.3
147	S	13.2	0.0110	10.321	0.36	36.3	66.5
185	Sa	10.4	0.0030	9.456	-0.49	38.4	60.8
193	-	15.4	-	-	-	-	68.0
214	S	12.5	0.0110	10.504	0.26	36.2	68.3
257	Sc	12.1	0.0053	9.976	0.27	35.0	64.0
258	Sa?	12.9	0.0140	10.493	0.41	35.0	70.5
288	Sb	8.9	0.0019	9.862	-0.34	30.2	77.0
291	SB	12.6	0.0070	9.851	0.04	36.6	79.0
301	S	14.4	0.0220	10.601	0.56	31.0	120.0
312	-	13.7	0.0180	10.788	0.60	44.1	71.2
342	Sc	11.6	0.0044	10.151	0.35	33.6	71.5
351	-	14.3	0.0130	10.671	0.97	35.0	67.5
365	Sc	10.9	0.0020	9.758	0.36	32.0	73.2
368	Sb	13.4	0.0020	8.681	0.28	32.1	97.7
381	-	14.9	0.0230	10.953	1.03	42.5	60.8
393	Sb	12.0	0.0030	9.426	0.12	31.0	93.7
409	-	15.2	0.0210	10.588	0.95	38.3	77.2
428	pec	12.9	0.0050	9.632	0.24	35.0	70.2
432	SB0	14.1	0.0190	10.939	0.78	39.7	70.7
449	S pec	11.9	0.0090	10.466	0.07	34.9	68.8
490	comp	14.3	0.0350	11.108	0.89	36.7	71.0
497	-	13.6	0.0070	9.650	0.24	42.8	70.0
517	S pec	13.5	0.0160	10.490	0.33	34.4	72.7
534	Sab	13.9	0.0170	10.964	0.90	33.7	74.0
536	S pec	14.4	0.0260	10.828	0.61	34.2	78.0
538	-	15.4	0.0190	10.699	1.15	37.7	69.2
541	S pec	13.9	0.0220	10.921	0.64	35.7	65.8
564	SB	14.4	0.0254	10.726	0.54	44.7	90.7
585	S comp	14.3	0.0171	10.855	0.92	34.5	67.8

Table 1 (continued)

AKN	$fr^W_{60\mu m}$	$fr^W_{100\mu m}$	T_d(12/25) [K]	$T^W_{12,25}$ [K]	$fr^W_{25\mu m}$	L^W_{FIR}/L_{FIR} n=1	L^W_{FIR}/L_{FIR} n=0
55							
77	0.44	0.12	173	198	0.67	0.45	-
80	0.48	0.15	161	186	0.63	0.47	-
88	0.61	0.23	168	190	0.68	0.58	0.74
89	0.62	0.23	166	184	0.73	0.61	0.76
120	0.42	0.07	200	208	0.95	0.79	0.85
136	0.64	0.26	169	194	0.65	0.61	0.76
147	0.53	0.18	190	224	0.65	0.54	0.71
185	0.65	0.28	180	226	0.54	0.61	0.77
193	0.81	0.44	-	217	0.79	-	-
214	0.53	0.17	181	207	0.68	0.54	0.70
257	0.46	0.14	162	202	0.50	0.42	0.62
258	0.46	0.13	189	217	0.69	0.50	0.66
288	0.10	0.02	174	292	0.27	0.13	0.37
291	0.28	0.06	202	238	0.69	0.40	0.58
301	0.25	0.04	201	212	0.92	0.61	0.69
312	0.78	0.38	149	158	0.84	0.77	0.88
342	0.36	0.09	179	212	0.62	0.39	0.59
351	0.46	0.14	185	221	0.62	0.47	0.65
365	0.23	0.05	199	278	0.46	0.29	0.51
368	0.22	0.04	187	202	0.83	0.45	0.60
381	0.78	0.43	186	222	0.62	0.75	0.88
393	0.12	0.02	193	237	0.60	0.26	0.47
409	0.60	0.19	198	214	0.84	0.70	0.80
428	0.45	0.12	194	226	0.68	0.50	0.66
432	0.67	0.26	156	167	0.80	0.66	0.79
449	0.45	0.13	187	219	0.65	0.47	0.65
490	0.54	0.17	204	233	0.75	0.61	0.74
497	0.75	0.35	208	230	0.81	0.80	0.88
517	0.42	0.11	210	247	0.70	0.51	0.66
534	0.36	0.08	174	198	0.68	0.40	0.59
536	0.40	0.09	212	240	0.77	0.55	0.68
538	0.59	0.21	186	208	0.74	0.62	0.76
541	0.50	0.16	234	300	0.62	0.56	0.72
564	0.76	0.30	166	170	0.94	0.85	0.91
585	0.43	0.12	182	218	0.61	0.44	0.63

4. DISCUSSION

The members of the subset have been plotted on the two-color diagram $\log(f_{60}/f_{100})$ against $\log(f_{12}/f_{25})$, which is presented in Fig. 9. Helou's (1986) model has been superimposed there.

With exception of the galaxies with Seyfert-like nuclei, the far IR radiation is a result of thermal reradiation from interstellar dust grains heated by starlight. The FIR model, proposed by Helou (1986), consists of two components - a cirrus-like one and a warm one, connected with active star forming regions. To trace curve D in his

paper, Helou (1986) used an estimation made by Desert (1986) of the emission from dust particles of various sizes and convenient heating radiation field. The last one was altered from an intensity comparable to the solar neighbourhood (point X), to one similar to the intensity found in the regions of active star formation (point Y). The other curve H was computed from Helou's (1986) two-component model and it represents the locus of points in the color-color diagram, where the contributions from the warm and cool components are equal.

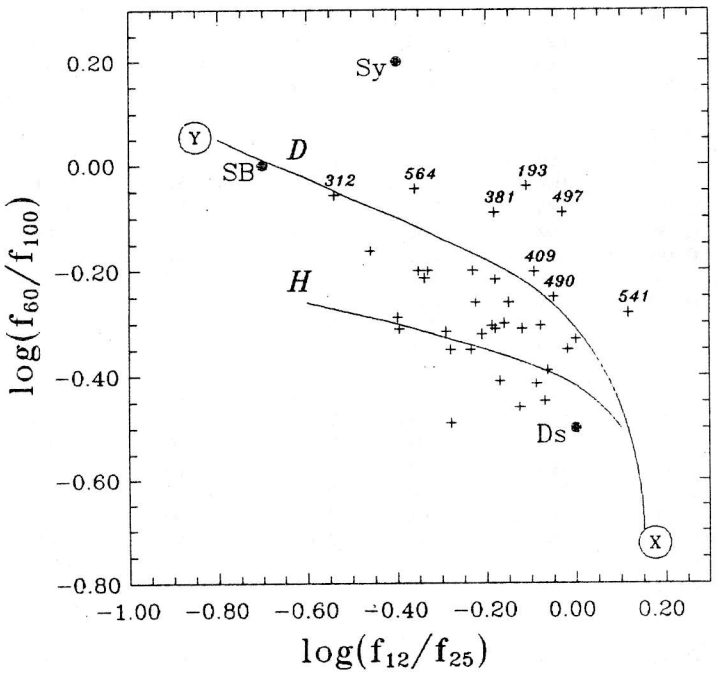

Fig. 9. *IR color-color diagram $\log(f_{60}/f_{100})$ against $\log(f_{12}/f_{25})$. Helou's (1986) model is superimposed there. The circles labelled as SB and SyG mark the colors of the "starburst" and "Seyfert" components adopted by Rowan-Robinson (1986). See text for more details.*

Most of the galaxies on this diagram, where the ratio L_{IR}/L_B increases from the lower right to the upper left corner, are placed between curves D and H. This indicates that the *IRAS*-detected AKNs are objects with enhanced star formation rate.

The objects lying definitely above the line D on the Helou diagram have been considered as the most interesting ones in the subset. These will be listed below in more details. In Table 1 their names are given in bold. The abbreviations in cross-references of their names refer to the following catalogues or surveys: N=NGC (Dreyer, 1888), I = IC (Dreyer, 1908), A = Second Reference Catalogue of Bright Galaxies (Vaucouleurs et al., 1976) - anonymous galaxy, U - UGC (Nilson, 1973), Mk =

Markarian Survey (Markarian, 1967; Markarian et al., 1981), Zw, ZwG = Zwicky compact galaxy (Zwicky, 1971), MCG = Morphological Catalogue of Galaxies (Vorontzov-Veliaminov et al., 1962-1964).

Akn 193 - an object with unknown redshift. According to *IRAS* fluxes the warm fractions are $fr^{W}_{60\mu m}$ = 0.81 and $fr^{W}_{25\mu m}$ = 0.79. On the color-color diagram $\alpha(60/100)$ vs $\alpha(25/60)$ given by SM, where different types of ELGs are presented, this galaxy lies in the starburst region.

Akn 312 = U 6665 = Mk 1304. An elliptical object with a jet (Arakelian, 1975), whose optical emission lines are very bright (Doroshenko and Terebizh, 1975). Akn 312 lies just on the curve D in the region with high SFR. Its total IR emission is about $6\cdot10^{10}\cdot L_{\odot}$ and the corresponding warm fraction is 0.78. On SM diagram this object is situated in the starburst region.

Akn 381=I 3581. An elliptical blue object with an envelope, showing medium H_{α} emission and weak [NII] $\lambda\lambda$ 6548/83 one (Arakelian et al., 1976). Its vigorous IR radiation $L_{FIR}\sim 9\cdot10^{10}\ L_{\odot}$ exceeds nearly 6 times the luminosity in the blue visual band. The corresponding warm IR fraction is about 0.75. But on SM diagram this galaxy lies definitely below the starburst region.

Akn 409 = ZwG 217.024 = MCG 07-27-056. A compact elliptical object, showing strong H_{α} and medium [NII], [SII] optical emissions (Arakelian et al., 1976). On the Helou diagram Akn 409 lies above the line D. It shows a strong IR emission $L_{FIR}\sim 4\cdot10^{10}L_{\odot}$ and the corresponding warm fraction is about 0.7. This galaxy is well situated on the SM diagram just in the starburst region.

Akn 490 = I Zw 129 = A 1554+42 = U 10099 = MCG 07-33-016 = Mk 1101. A quite symmetric blue object, which shows strong H_{α} and medium [NII] optical emissions (Arakelian et al., 1976). Akn 490 is well situated in starburst region on SM diagram too. The IR emission is very strong - about $1.3\cdot10^{11}\ L_{\odot}$. The estimation of its warm fraction is 0.61.

Akn 497 = U 10200 = MCG 07-33-039 = Mk 1104. A compact object with non-symmetrical red envelope which shows strong H_{α} and weak [NII] emissions (Arakelian et al., 1976). The IR emission is relatively weak - about $5\cdot10^{9}L_{\odot}$, and the corresponding warm fraction connected with starburst events is 0.8. The IR properties of Akn 497 are very similar to those of Akn 490, the former object discussed.

Akn 541 = I 4763 = U 11290. A peculiar very blue spiral with strong H_{α} and medium [NII] emission (Arakelian et al., 1976). The total FIR emission $L_{FIR}\sim 8\cdot10^{10}L_{\odot}$ exceeds about 4.5 times its blue luminosity. The corresponding warm IR fraction is 0.56.

Akn 564 = A 2240+29 = U 12163 = MCG 05-53-012. A well known Seyfert galaxy, showing strong and wide (about 100 A) H_{α} emission (Arakelian et al., 1976). About 0.85 of its IR emission is due to the starburst processes. On SM diagram this galaxy lies definitely in the Seyfert region.

All of the above mentioned objects call for more attention because of their vigo-

rous IR luminosities and their fairly large warm fractions, which are intimately associated with the starburst activity. All these galaxies are blue compact objects, showing rather strong optical low-excitation emission-line spectra. It seems to be very likely they all are starburst galaxies. There are good reasons to intend a more comprehensive observational program to investigate them in more details.

5. CONCLUSIONS

On the basis of the discussion above the following conclusions have been made:

1. About 63% of *IRAS*-detected AKNs show high total IR luminosities $L_{FIR} \geq 10^{44}$ erg·s^{-1} in 1-500 μm IR spectral region.

2. The distribution of $\log(f_{60}/f_{100})$ shows that the *IRAS* AKNs are warmer than the "normal" S galaxies with a clear peak at about T=45 K (n=0 model). The temperature color index f_{60}/f_{100} of *IRAS* AKNs is distributed similarly to that of the BCELGs.

3. *IRAS*-selected AKNs tend to extend the relation f_{100}/f_{60} vs L_{IR}/L_B for "normal" S galaxies and emit up to seven times more energy in the IR spectral band between 40 and 120 μm. Its mean ratio $\langle L_{FIR}/L_B \rangle$ of FIR luminosities to blue ones is about 3.63.

4. It is very likely that in *IRAS*-detected AKNs there are two IR components - warm one, connected with the UV fluxes of new-born massive stars, reradiated by dust, and cool one, originated from dust in galactic disks, which is heated by the general interstellar radiation field. The ability to deduce total warm IR luminosities L^W_{FIR} and warm IR fractions L^W_{FIR}/L_{FIR} rests on IR color-color diagrams $\alpha(25/12)$, $\alpha(60/25)$ and $\alpha(100/60)$. The mean warm IR fraction is $\langle L^W_{FIR}/L_{FIR} \rangle \approx 0.55$, if the grain mass absorption coefficient is n=1.0, or $\langle L^W_{FIR}/L_{FIR} \rangle \approx 0.72$ if n=0.0.

5. If the dust clouds are optically thin, the dust mass of *IRAS*-detected AKNs, which is responsible for IR flux densities observed at 60 μm, is derived to be $\mathfrak{M}_{dust}(60\ \mu m) \sim 10^5\ \mathfrak{M}_\odot$.

6. There is a correlation between L_{IR} and L_B, which indicates that the most *IRAS*-detected AKNs have enhanced rather than constant star formation rate.

Acknowledgements

We would like to thank A.I.Shapovalova for her stimulating discussion of this work.

REFERENCES

Arakelian M.A.: 1975, *Soobshch. Byurakan Obs.*, **47**, 1.
Arakelian M.A., Dibay E.A., Yesipov V.F.: 1975, *Astrofizika*, **11**, 195.
Arakelian M.A., Dibay E.F., Yesipov V.F.: 1976a, *Astrofizika*, **12**, 195.
Arakelian M.A., Dibay E.A., Yesipov V.F.: 1976b, *Astrofizika*, **12**, 683.

Belfort P., Mochkovitch R., Dennefeld M.: 1987, *Astron. Astrophys.*, **176**, 1.

de Vaucouleurs G., de Vaucouleurs A., Corwin N.C.: 1976, *The Second Reference Catologue of Bright Galaxies*, Austin, *University of Texas Press.*

Dennefeld M., Karoji H., Belfort P.: 1985, *in: Star-Forming Dwarf Galaxies and Related Objects*, eds. D. Kunth, T.X. Thuan, J. Tran Thanh Van, *Editions Frontieres*, Paris, 351.

Desert F.X.: 1986, *in: Light on Dark Matter*, ed. F.R. Israel, Reidel, Dordrecht, 213.

Dibay E.A., Doroshenko V., Terebizh V.: 1976, *Astrofizika*, **12**, 689.

Doroshenko V., Terebizh V.: 1975, *Astrofizika*, **11**, 631.

Draine B.T., Lee H.M.: 1984, *Astrophys. J.*, **285**, 89.

Dreyer J.L.E.: 1888, *Mem. R. Astron. Soc.*, **49**, 1.

Dreyer J.L.E.: 1908, *Mem. R. Astron. Soc.*, **59**, 1.

Gallagher J.S., Hunter D.A.: 1987, in: *Star Formation in Galaxies*, ed. Carol J. Lonsdale Persson, *NASA Conf. Publ.*, No. 2466, 167.

Harvit M., Houck J.R., Soifer B.T., Palumbo G.G.C.: 1987, in: *Star Formation in Galaxies*, ed. Carol J. Lonsdale Persson, *NASA Conf. Publ.*, No. 2466, 387.

Helou G.: 1985, in: *Star-Forming Dwarf Galaxies and Related Objects*, eds. D. Kunth, T.X. Thuan, J. Tran Thanh Van, *Editions Frontieres*, Paris, 319.

Helou G.: 1986, *Astrophys. J. Lett.*, **311**, L33.

Houck J.K., Soifer B.T., Neugebauer G., Beichman C.A., Aumann H.H. et al.: 1984, *Astrophys. J. Lett.*, **278**, L63.

Jong T. de, Clegg P.E., Soifer B.T., Rowan-Robinson M., Habing H., Houck J., Aumann H.H., Raimond E.: 1984, *Astrophys. J. Lett.*, **278**, L67.

Kunth D., Sevre F.: 1985, in: *Star-Forming Dwarf Galaxies and Related Objects*, eds.: D. Kunh, T.X. Thuan, J. Tran Thanh Van, *Editions Frontieres*, Paris, 331.

Lonsdale C.J., Helou G., Good J.C., Rice W., preparers: 1985, *Cataloged Galaxies and Quasars Observed in the IRAS Syrvey*, Jet Propulsion Laboratory, Pasadena.

Markarian B.E.: 1967, *Astrofizika*, **3**, 55.

Markarian B.E., Lipovetsky V.A., Stepanian J.A.: 1981, *Astrofizika*, **17**, 619.

Nilson P.: 1973, *Uppsala General Catalogue of Galaxies, Uppsala Obs. Ann.*, **6**.

Rowan-Robinson M.: 1987, in: *Star Formation in Galaxies*, ed. Carol J. Lonsdale Persson, *NASA Conf. Publ., No.* **2466**, *133.*

Salzer J., MacAlpine G.: 1988, *Astron. J.*, **96**, 1192 (SM).

Sekiguchi K.: 1987, *Astrophys. J.*, **316**, 145.

Soifer B.T., Houck J.R., Neugebauer G.: 1987, *Ann. Rev. Astron. Astrophys.*, **25**, 187.

Vorontzov-Veliaminov B.A., Krasnogorskaja A., Arkhipova V.: 1962-1964, *Morphological Catalogue of Galaxies, Moscow State University Publ.*, Moscow.

Zwicky F.: 1971, *Catalogue of Selected Compact Galaxies and Post-Eruptive Galaxies*, Guemligen.

Zwicky F., Herzog E., Wild P., Kowal C.: 1961-1968, *Catalogue of Galaxies and Clusters of Galaxies*, California Institute of Technology, Pasadena.